Published in final edited form as:
J Cogn Sci (Seoul). 2011 ; 12(2): 127–210.

Quantification of Load Dependent Brain Activity in Parametric N-Back Working Memory Tasks using Pseudo-continuous Arterial Spin Labeling (pCASL) Perfusion Imaging

Qihong Zou[1,2], **Hong Gu**[3], **Danny J.J. Wang**[4], **Jia-Hong Gao**[5,6], and **Yihong Yang**[7]

[1]MRI Research Center and Beijing City Key Lab for Medical Physics and Engineering, Peking University zouqihong@gmail.com; zouq@mail.nih.gov

[2]Neuroimaging Research Branch, National Institute on Drug Abuse, NIH zouqihong@gmail.com; zouq@mail.nih.gov

[3]Neuroimaging Research Branch, National Institute on Drug Abuse, NIH HGu@intra.nida.nih.gov

[4]Department of Neurology, University of California Los Angeles JJ.Wang@loni.ucla.edu

[5]MRI Research Center and Beijing City Key Lab for Medical Physics and Engineering, Peking University jgao@uchicago.edu

[6]Brain Research Imaging Center, University of Chicago jgao@uchicago.edu

[7]Neuroimaging Research Branch, National Institute on Drug Abuse, NIH yihongyang@intra.nida.nih.gov

Abstract

Brain activation and deactivation induced by N-back working memory tasks and their load effects have been extensively investigated using positron emission tomography (PET) and blood-oxygenation level dependent (BOLD) functional magnetic resonance imaging (fMRI). However, the underlying mechanisms of BOLD fMRI are still not completely understood and PET imaging requires injection of radioactive tracers. In this study, a pseudo-continuous arterial spin labeling (pCASL) perfusion imaging technique was used to quantify cerebral blood flow (CBF), a well understood physiological index reflective of cerebral metabolism, in N-back working memory tasks. Using pCASL, we systematically investigated brain activation and deactivation induced by the N-back working memory tasks and further studied the load effects on brain activity based on quantitative CBF. Our data show increased CBF in the fronto-parietal cortices, thalamus, caudate, and cerebellar regions, and decreased CBF in the posterior cingulate cortex and medial prefrontal cortex, during the working memory tasks. Most of the activated/deactivated brain regions show an approximately linear relationship between CBF and task loads (0, 1, 2 and 3 back), although several regions show non-linear relationships (quadratic and cubic). The CBF-based spatial patterns of brain activation/deactivation and load effects from this study agree well with those obtained from BOLD fMRI and PET techniques. These results demonstrate the feasibility of ASL techniques to quantify human brain activity during high cognitive tasks, suggesting its potential application to assessing the mechanisms of cognitive deficits in neuropsychiatric and neurological disorders.

Keywords

N-back working memory; cerebral blood flow; load effects; pseudo-continuous arterial spin labeling (pCASL)

1. Introduction

N-back working memory tasks have been widely used as high-level cognitive tasks in positron emission tomography (PET) (Jonides et al., 1997) and blood-oxygenation level dependent (BOLD) functional magnetic resonance imaging (fMRI) (Braver et al., 1997; Cohen et al., 1997; Owen, McMillan, Laird, & Bullmore, 2005; Tomasi, Ernst, Caparelli, & Chang, 2006; Veltman, Rombouts, & Dolan, 2003) studies, in which subjects are instructed to monitor the identity of a series of stimuli and to respond when the currently presented stimulus is the same as the one presented N trials previously. It is known that N-back working memory tasks induce brain activation in a large-scale network including fronto-parietal cortices, thalamus, basal ganglia and cerebellum (Braver et al., 1997; Cohen et al., 1997; Jonides et al., 1997; Owen et al., 2005; Tomasi et al., 2006; Veltman et al., 2003). Consistent findings of brain deactivation induced by N-back working memory tasks were shown at the posterior cingulate cortex and medial prefrontal cortex (Greicius, Krasnow, Reiss, & Menon, 2003; Hampson, Driesen, Skudlarski, Gore, & Constable, 2006; Jonides et al., 1997; Tomasi et al., 2006). These tasks have been widely used in various clinical studies including Alzheimer's disease (Kensinger, Shearer, Locascio, Growdon, & Corkin, 2003), mild cognitive impairment (Bokde et al., 2010), Schizophrenia (Callicott et al., 2003) and attention deficit hyperactivity disorder (Valera, Faraone, Biederman, Poldrack, & Seidman, 2005). Further, load effects of parametric N-back working memory tasks on brain activation as measured by PET (Jonides et al., 1997) and BOLD fMRI (Braver et al., 1997; Cohen et al., 1997; Tomasi et al., 2006; Veltman et al., 2003) have been demonstrated in the fronto-parietal cortices, thalamus and cerebellum. Load effects of parametric N-back working memory tasks on brain deactivation as measured by PET (Jonides et al., 1997) and BOLD fMRI (Tomasi et al., 2006) have also been reported in the posterior cingulate cortex and medial prefrontal cortex. Abnormal load effects of parametric N-back working memory tasks on brain activation have been reported in clinical populations such as Schizophrenia (Callicott et al., 2003).

However, BOLD signal results from changes in cerebral blood flow (CBF), cerebral blood volume, and cerebral oxygen consumption near the activated brain region (Ogawa et al., 1993), and its role as a surrogate of neuronal activity is still under investigation. Alternatively, arterial spin labeling (ASL) perfusion imaging techniques use CBF, a well understood physiological parameter, as an indicator of neuronal activity (Detre, Leigh, Williams, & Koretsky, 1992; Williams, Detre, Leigh, & Koretsky, 1992). Similar to PET, ASL fMRI can provide quantitative measurement of CBF (Detre et al., 1992; Williams et al., 1992). In contrast to PET, which requires radioactive tracer injection, ASL fMRI provides CBF measurement by using magnetically labeled blood water as an endogenous tracer (Detre et al., 1992; Williams et al., 1992). Moreover, evidence suggests that ASL fMRI has less inter-subject variability than BOLD fMRI (Wang et al., 2003), which might improve statistical power in group analysis. Reduced susceptibility effects in brain regions with severe magnetic field inhomogeneity (Wang et al., 2004), and high spatial specificity compared to BOLD fMRI (Duong, Kim, Ugurbil, & Kim, 2001; Luh, Wong, Bandettini, Ward, & Hyde, 2000) have also been demonstrated using ASL fMRI. In addition, ASL techniques provide quantitative measurements at both baseline and activated states, and therefore should help to interpret data in which signals in both states are important, while results solely from BOLD fMRI with percentage signal changes between the two states should be interpreted with caution (Fleisher et al., 2009). Due to these potential advantages, ASL fMRI may provide a valuable tool in the investigation of brain function in both basic and clinical neuroscience.

However, most existing ASL fMRI studies have been conducted using sensorimotor (Garraux, Hallett, & Talagala, 2005; Mildner et al., 2003; Wang, Aguirre, Kimberg, &

Detre, 2003; Wang, Aguirre, Kimberg, Roc et al., 2003; Yang et al., 2000) and visual (Aguirre, Detre, Zarahn, & Alsop, 2002; Talagala & Noll, 1998; Yang et al., 2000) tasks. Only a handful of ASL studies have been conducted to study higher cognition, including verb generation (Yee et al., 2000), motor learning (Olson et al., 2006), psychological stress (Wang, Rao et al., 2005), natural vision (Rao, Wang, Tang, Pan, & Detre, 2007), time-on-task effect (Lim et al., 2010), memory encoding tasks (Bangen et al., 2009; Xu et al., 2010), arithmetic task (Lin, Hasson, Jovicich, & Robinson, 2011) and N-back working memory tasks (Kim et al., 2006; Pfefferbaum et al., 2011; Ye et al., 1998). With respect to N-back working memory tasks using ASL fMRI, Ye and colleagues (Ye et al., 1998) employed a single-slice acquisition during a 2 back (2b) working memory task and demonstrated the feasibility of investigating brain activation during working memory tasks. Later on, Kim and colleagues (Kim et al., 2006) conducted a multi-slice whole-cerebral cortex study during a 2b working memory task and showed widespread activation in fronto-parietal networks. Recently, Pfefferbaum and colleagues (Pfefferbaum et al., 2011) demonstrated decreased CBF in the posterior cingulate, posterior-inferior precuneus, and medial frontal lobes during a spatial working memory task. However, no studies have systematically studied the brain activation and deactivation induced by parametric N-back working memory tasks and the corresponding load effects based on quantitative CBF using ASL fMRI.

In the current study, using a pseudo-continuous ASL (pCASL) technique (Dai, Garcia, de Bazelaire, & Alsop, 2008; Wu, Fernandez-Seara, Detre, Wehrli, & Wang, 2007), we acquired fMRI data during parametric N-back [0, 1, 2 and 3 back (0b, 1b, 2b, 3b)] working memory tasks on a relatively large sample (n = 40). We quantif CBF in the baseline (0b) and task (1b, 2b, and 3b) states in the activated and deactivated brain regions and assessed the load effects based on quantitative CBF.

2. Materials and methods

2.1 Participants

Forty healthy volunteer (mean ± S.D. 27.5 ± 8.2 years old, 21 females) participated in the study. All subjects were screened with a questionnaire to ensure no history of neurological illness, psychiatric disorders or past drug abuse. They were recruited under a protocol approved by the Institutional Review Board of the Intramural Research Program of the National Institute on Drug Abuse. Signed informed consent was obtained from all participants prior to study enrollment.

2.2 Experimental paradigm

Participants underwent block-design N-back working memory tasks. Visual stimuli were presented and responses were collected using E-Prime (Psychology Software Tools, Inc.). The stimuli were back-projected on a screen inside the scanner using an LCD projector. The task was presented as a block paradigm with four conditions: three active working memory tasks (1b, 2b, 3b) and a baseline vigilance task (0b). Each 62-sec block consists of a 2-sec instruction indicative of the task difficulty followed by 30 consecutive trials of single letter stimuli (500 ms duration, 1500 ms ISI). In the baseline vigilance task, following the instruction “press for D”, participants pressed one button each time the letter D (or d) appeared on the screen. In the three active working memory task conditions, following the instruction “N back” (N can be “one,” “two,” and “three”), participants pressed one button when the letter showing on the screen matched the one presented “N” items back. The task included 6 runs, with one 0b, 1b, 2b or 3b block in each run and took a total of approximately 27 minutes. Each run lasted 4 minutes and 24 seconds, beginning with a 16-sec fixation and a 0b; all 6 possible orders of 1b, 2b and 3b were used in the 6 runs, with the run order randomized across participants. The primary behavioral performance

measurements at each task condition level were hit rate, false alarm rate and dprime. Hit rate is the proportion of trials that a subject should give a button-press response, to which the subject responded to these trails correctly. False alarm rate is the proportion of trials that a subject should not give a button-press response, to which the subject responded to these trials anyway. The dprime is a measurement of hit rate while penalizing for the false alarm rate, which can be calculated as the difference between the z-transforms of these 2 rates using the following equation: dprime = *z*(hit rate) – *z*(false alarm rate).

2.3 Data acquisition

Functional MRI data were collected on a 3-T Siemens Allegra MR scanner (Siemens, Erlangen, Germany) equipped with a quadrature volume head coil. Head movement was minimized by using a polyurethane foam helmet individually made for each participant. A pseudo continuous arterial spin labeling (pCASL) technique (Dai et al., 2008; Wu et al., 2007) was employed for cerebral blood flow (CBF) measurement. Interleaved control and label images were acquired using a gradient echo EPI sequence with the following parameters: TR/TE = 4000/13 ms, FA = 90°, slice thickness = 5mm with 20 % gap, 20 slices, FOV = 220 × 220 mm^2 with in-plane resolution of 3.44 × 3.44 mm^2, labeling duration = 1.6 s, label offset = 80 mm, post-labeling delay = 1.2 s and bipolar gradient with b = 2 sec/mm^2. For registration purposes, a set of high-resolution anatomical images were acquired using a 3-D magnetization prepared rapid gradient echo (MPRAGE) T_1-weighted sequence (256 × 192 × 160 matrix size; 1 × 1 × 1 mm^3 in-plane resolution; TI/TR/TE = 1000/2500/4.38 ms; flip angle = 8°) on each participant.

2.4 Data processing

The pCASL data were preprocessed using the Analysis of Functional Neuroimaging (AFNI) software package (Cox, 1996). The number of outliers in the control and label images were counted separately using the program *3dToutcount* implemented in AFNI. A pair of control and label images with the fewest outliers was chosen as base for motion correction and were linearly registered to each other. Then control and label images were registered to their base separately. Following head motion correction, images were spatially smoothed with a 6-mm Gaussian kernel, and label images were subtracted from control images to get CBF-weighted time series. The control images and CBF-weighted images were extracted for each working memory condition based on the task design of for each subject. Quantitative CBF maps for all the four working memory conditions were generated using one-compartment model (Wang, Zhang et al., 2005) as the following equation:

$$f=\frac{\lambda\,\Delta MR_{1a}}{2\alpha M_{con}\left\{\exp\left(-w\,R_{1a}\right)-\exp\left[-\left(\tau+w\right)R_{1a}\right]\right\}},$$

where λ (0.9 ml/g) is the blood-tissue water partition coefficient, ΔM is the average intensity of CBF-weighted time series under that working memory condition, R_{1a} (0.67 sec^{-1}) is the longitudinal relaxation rate of blood, α (80%) is the tagging efficiency, M_{con} is the average intensity of control images under that working memory condition, w (1.2 sec) is the post-labeling delay time, and τ (1.6 sec) is the duration of the labeling pulse. Finally, the working memory task CBF maps of each subject were coregistered with the corresponding anatomical maps and spatial normalized to standard Talairach and Tournoux (TT) space with a resampling resolution of 3 × 3 × 3 mm^3 to facilitate group analysis.

2.5 Statistical analysis

Paired t-tests were conducted on the whole brain CBF values between each pair of the four conditions, including 0b, 1b, 2b and 3b. Significance threshold for paired t-test on whole brain CBF values were set at $p < 0.05$.

To show the general activation and deactivation patterns of working memory tasks, paired t-tests were conducted between the three active working memory tasks (1b, 2b and 3b) and the baseline vigilance task (0b). Trend analyses, including linear, quadratic and cubic trends, were conducted across the four working memory conditions based on quantitative CBF. To control Type I error in the resultant voxel-wise maps of paired t-test and trend t-tests, Monte Carlo simulations were performed using the AFNI AlphaSim program. By iterating the process of random image generation, spatial correlation of voxels, thresholding and cluster identification, the program provides an estimate of the overall significance level achieved for various combinations of individual voxel probability threshold and cluster size threshold (Poline, Worsley, Evans, & Friston, 1997). Using this program, a corrected significance level of $p < 0.05$ for the resultant statistical maps was obtained by clusters with a minimum volume of 2052 mm^3 at an uncorrected individual voxel height threshold of $p < 0.01$.

Regions of interest (ROI) for the task positive network and task negative network were generated from a corrected paired *t*-map. ROIs for posterior cingulate cortex, medial prefrontal cortex, anterior temporal gyrus, inferior parietal lobule (IPL), middle frontal gyrus, dorsolateral prefrontal cortex, anterior insula, supplementary motor area, left precentral gyrus, thalamus, caudate, cerebellum/fusiform gyrus and vermis were generated from a corrected linear trend *t*-map. We also generated bilateral IPL regions that showed a quadratic trend of activations and a right IPL region that showed cubic trend of activation based on the corrected quadratic and cubic trend *t*-maps. Average CBF values in each ROI across the four working memory conditions were shown to demonstrate the load effects.

3. Results

3.1 Behavioral data

The behavioral data of N-back working memory tasks are shown in Table 1. Hit rate decreases with increasing task load from 0b to 3b (Linear trend: $t = -16.16$, $p = 7.0 \times 10^{-19}$; quadratic trend: $t = 5.34$, $p = 4.2 \times 10^{-6}$; cubic trend: $t = 2.74$, $p = 9.2 \times 10^{-3}$). False alarm rate increases with increasing task load (Linear trend: $t = 6.52$, $p = 9.9 \times 10^{-8}$; quadratic trend: $t = 3.26$, $p = 2.3 \times 10^{-3}$; cubic trend: $t = 2.60$, $p = 1.3 \times 10^{-2}$), while dprime linearly decreases with increasing task load ($t = -29.54$, $p = 3.0 \times 10^{-28}$).

3.2 N-back working memory task load effects on whole brain CBF

Whole brain CBF values across the four working memory task conditions were shown in Table 2. ANOVA analysis showed significant working memory load effect on whole brain CBF ($F3,117 = 2.96$, $p = 0.035$). Compared across the four working memory conditions, the only significant impact of working memory task load on whole brain CBF was observed between 3b and 0b, where whole brain CBF was significantly higher under 3b than under 0b ($p = 0.011$, uncorrected; i.e. $p = 0.066$, corrected). This observation is in consistent with the notion mentioned by Raichle (Raichle, 2006) that the additional energy burden associated with momentary demands of the environment may be as little as 0.5 to 1.0% of the total energy budget (Raichle & Mintun, 2006), while most energy is consumed by intrinsic resting-state activity.

3.3 Working memory task activation and deactivation

Task activation and deactivation comparing the three active working memory tasks and the baseline vigilance task are shown in Fig. 1. Task activation under 3b compared to 0b was observed in the inferior parietal lobule, middle frontal gyrus, supplementary motor area, precentral gyrus, dorsolateral prefrontal cortex, superior parietal lobule, anterior insula, precuneus, caudate, thalamus and cerebellum. On the other hand, task deactivation under 3b compared to 0b was observed in the posterior cingulate cortex, medial prefrontal cortex, and anterior temporal gyrus (Fig. 1). Similar patterns of activation and deactivation were observed when comparing 2b or 1b to 0b. These results are generally in agreement with previous working memory data (Jonides et al., 1997; Kim et al., 2006; Owen et al., 2005; Tomasi et al., 2006).

3.4 N-back working memory task load effects on voxel-wise CBF

Fig. 2 shows the brain regions exhibiting the linear, quadratic and cubic trend contrasts (corrected $p < 0.05$). The regions that showed a linear increase of CBF with task loads were located at cortical regions including inferior parietal lobule, middle frontal gyrus, supplementary motor area, precentral gyrus, dorsolateral prefrontal cortex, superior parietal lobule, anterior insula and precuneus, subcortical regions including caudate, thalamus and cerebellum. The only regions that showed a linear decrease of CBF with task loads were located at cortical regions including PCC and MPFC. The regions that showed a quadratic trend of CBF were located at bilateral IPL. Right IPL activation also showed a cubic trend. No brain regions showed a significant quadratic or cubic trend of CBF in the task deactivated brain regions. Figs. 3 and 4 show the linear, quadratic and cubic trend of average CBF values in each ROI across the four working memory conditions.

4. Discussion

Using the pCASL technique with a whole cerebral-cortex coverage on a relatively large sample (n = 40), the current study systematically investigated the patterns of brain activation and deactivation induced by parametric N-back working memory tasks based on quantitative CBF. We showed that, comparing 3b with 0b, the fronto-parietal cortices, thalamus, caudate, and cerebellar regions were activated, while the posterior cingulate cortex and medial prefrontal cortex were deactivated. Further, we investigated the load effects of N-back working memory tasks on brain activity. The frontoparietal cortices, thalamus, caudate, and cerebellar regions showed a linear increasing trend of CBF from 0b to 3b, while the posterior cingulate cortex and medial prefrontal cortex showed a linear decreasing trend of CBF with task loads. In addition, the bilateral inferior parietal lobule exhibited a quadratic trend of CBF increase with task loads. The right inferior parietal lobule also showed cubic trend of CBF increase with task loads.

In general, N-back working memory tasks induced activation in the cortical, subcortical and cerebellar regions using the pCASL perfusion fMRI resembled the regions revealed from previous BOLD fMRI (Braver et al., 1997; Cohen et al., 1997; Owen et al., 2005; Tomasi et al., 2006; Veltman et al., 2003) and PET (Jonides et al., 1997) studies. The locations of task induced deactivation in the midline regions including the posterior cingulate cortex and medial prefrontal cortex were consistent with the findings from previous BOLD fMRI (Greicius et al., 2003; Hampson et al., 2006; Tomasi et al., 2006) and PET (Jonides et al., 1997) studies. In the current study, using pCASL technique (Dai et al., 2008; Wu et al., 2007) with both high labeling efficiency and signal-to-noise ratio, we replicated and substantially extended the findings from previous 2b working memory studies based on single-slice pulsed ASL (Ye et al., 1998) and multi-slice continuous ASL (Kim et al., 2006).

To the best of our knowledge, this is the first study to investigate the load effects of parametric N-back working memory tasks on brain activity based on quantitative CBF using pCASL. Our findings are in agreement with those measured by PET (Jonides et al., 1997) and BOLD fMRI (Braver et al., 1997; Cohen et al., 1997; Greicius et al., 2003; Hampson et al., 2006; Jansma, Ramsey, Coppola, & Kahn, 2000; Tomasi et al., 2006; Veltman et al., 2003), which are mainly located at the fronto-parietal cortices, thalamus, caudate, cerebellum, posterior cingulate cortex and medial prefrontal cortex.

This study demonstrates that the quantitative CBF increases linearly in the fronto-parietal cortices, thalamus, caudate and cerebellum from 0b to 3b task conditions. The load effect of brain activation within dorsolateral prefrontal cortex is consistent with its role in the active maintenance of information in working memory (Braver et al., 1997; Cohen et al., 1997). It has been suggested that the parietal cortices, basal ganglia, and supplementary motor area, in cooperation with Broca's area, are involved in verbal rehearsal, thus the load effect observed in these areas is consistent with the increase in number of rehearsal items associated with increasing load (Cohen et al., 1997). Jonides and colleagues (Jonides et al., 1997) assert that these fonto-parietal cortices, thalamus, caudate, and cerebellum respond to increased storage, rehearsal, matching, temporal ordering and inhibition processes required by higher task loads, separately. Jansma and colleagues (Jansma et al., 2000) argue that the load effect of N-back working memory tasks on brain activity might reflect increased manipulation of stimuli, rather than an increased load on temporary retention of stimuli.

We observed that the CBF decreased linearly in the posterior cingulate cortex and medial prefrontal cortex from 0b to 3b task conditions, which is consistent with previous PET (Jonides et al., 1997) and BOLD fMRI (Greicius et al., 2003; Hampson et al., 2006; Tomasi et al., 2006) studies. These two regions are key components of the default mode network (Raichle et al., 2001), and independently deactivated by goal-directed tasks (Binder et al., 1999; Mazoyer et al., 2001; Shulman et al., 1997). Resting-state functional connectivity (Greicius et al., 2003) findings show that the posterior cingulate cortex and medial prefrontal cortex temporally synchronize with each other. Furthermore, Fox and colleagues (Fox et al., 2005) have demonstrated that in resting state the posterior cingulate cortex and medial prefrontal cortex are negatively correlated, i.e. competing, with brain regions activated by working memory tasks. McKiernan and colleagues (McKiernan, Kaufman, Kucera-Thompson, & Binder, 2003) have proposed that during the parametric working memory tasks, when the resources are needed and reallocated to the activated brain regions such as the fronto-parietal cortices, the posterior cingulate cortex and medial prefrontal cortex are deactivated. Moreover, the deactivation magnitude increases with task difficulty (Jonides et al., 1997; McKiernan et al., 2003; Tomasi et al., 2006).

In addition, a nonlinear trend of CBF changes from 0b to 3b task conditions was observed. Quantitative CBF at the bilateral inferior parietal lobule exhibited a quadratic trend. Similarly, using a parametric Sternberg task, Kirschen and colleagues (Kirschen, Chen, Schraedley-Desmond, & Desmond, 2005) observed quadratic responses in the parietal lobe. Specifically, from visual inspection, we show that the quadratic trend is driven by the similar quantitative CBF activity between 2b and 3b task conditions, indicating that saturation/plateauing of working memory mechanisms might be involved above 2b working memory (Braver et al., 1997). In addition, quantitative CBF at the right inferior parietal lobule shows a cubic trend, but the underlying mechanism is not yet clear and warrants further investigation.

ASL fMRI techniques may have several advantages over BOLD fMRI and PET. ASL techniques provide quantitative CBF measurement with stable noise characteristics over the entire spectrum (Wang, Aguirre, Kimberg, & Detre, 2003) and are completely noninvasive,

in contrast to PET. CBF is potentially a better index of neural activity than BOLD, since it is a single physiological parameter (rather than an interplay of several parameters) and is sensitive to water exchange between intra- and extra-vascular compartments in capillary (rather than oxygenation in large veins). Miller and colleagues (Miller et al., 2001) suggest that the relation between CBF and neural activity may be more linear than the relation between BOLD and neural activity. CBF measurements with ASL fMRI have been shown to agree well with results from $H_2{}^{15}O$ PET (Ye et al., 2000). In addition, ASL may provide reduced motion and susceptibility artifacts in brain regions with severe magnetic field inhomogeneity (Wang et al., 2004), smaller inter-subject variance (Wang, Aguirre, Kimberg, Roc et al., 2003), and potentially greater spatial resolution (Duong et al., 2001; Luh et al., 2000). Moreover, ASL fMRI provides quantitative CBF measurements at both baseline and activated states, while results from BOLD fMRI studies with signal percentage change between activated and baseline states should be interpreted with caution. Fleisher and colleagues (Fleisher et al., 2009) found a decreased percentage signal change in an associative encoding task in an Alzheimer's disease high risk group compared to an Alzheimer"s disease low risk group, using both BOLD and ASL contrast. However, the baseline CBF in the high risk group was demonstrated to be abnormally elevated, while CBF under the associative encoding task is not significantly different between the high and low risk groups. Though the current ASL techniques still suffer from technical limitations such as fewer number of slices, lower temporal resolution and SNR, with continuing technical improvements to come, ASL fMRI is expected to be increasingly used for clinical studies, such as schizophrenia and Alzheimer's disease. The current study, which demonstrates the feasibility of using ASL fMRI for investigating brain activity induced by parametric N-back working memory tasks, may inspire further applications of this technique to patient populations with cognitive abnormalities.

5. Conclusions

In this study we systematically investigated the brain activation and deactivation induced by parametric N-back working memory tasks and the corresponding load effects. The spatial patterns of brain activation and deactivation and load effects detected by pCASL fMRI are consistent with previous findings by BOLD fMRI and PET, indicating the feasibility of pCASL to investigate higher order cognitive brain functions. Furthermore, ASL provides more quantitative measurement than BOLD, while it is completely noninvasive in contrast to PET. Our findings suggest potential applications of ASL fMRI techniques, with advantages of quantitative measurements at both baseline and activated states, to the assessment of neuropsychiatric and neurological populations with cognitive deficits.

Acknowledgments

This work was supported by the Intramural Research Program of the National Institute on Drug Abuse (NIDA), National Institutes of Health (NIH). This work was also supported by NIH grants MH080892 and MH080892-S1, and by a China"s national strategic basic research program (""973"") grant 2012CB720702. The authors thank Dr. Yufeng Zang and Dr. Thomas J. Ross for helpful discussions.

References

Aguirre GK, Detre JA, Zarahn E, Alsop DC. Experimental design and the relative sensitivity of BOLD and perfusion fMRI. Neuroimage. 2002; 15(3):488–500. [PubMed: 11848692]

Bangen KJ, Restom K, Liu TT, Jak AJ, Wierenga CE, Salmon DP, et al. Differential age effects on cerebral blood flow and BOLD response to encoding: associations with cognition and stroke risk. Neurobiol Aging. 2009; 30(8):1276–1287. [PubMed: 18160181]

Binder JR, Frost JA, Hammeke TA, Bellgowan PS, Rao SM, Cox RW. Conceptual processing during the conscious resting state. A functional MRI study. J Cogn Neurosci. 1999; 11(1):80–95. [PubMed: 9950716]

Bokde AL, Karmann M, Born C, Teipel SJ, Omerovic M, Ewers M, et al. Altered brain activation during a verbal working memory task in subjects with amnestic mild cognitive impairment. J Alzheimers Dis. 2010; 21(1):103–118. [PubMed: 20413893]

Braver TS, Cohen JD, Nystrom LE, Jonides J, Smith EE, Noll DC. A parametric study of prefrontal cortex involvement in human working memory. Neuroimage. 1997; 5(1):49–62. [PubMed: 9038284]

Callicott JH, Mattay VS, Verchinski BA, Marenco S, Egan MF, Weinberger DR. Complexity of prefrontal cortical dysfunction in schizophrenia: more than up or down. Am J Psychiatry. 2003; 160(12):2209–2215. [PubMed: 14638592]

Cohen JD, Perlstein WM, Braver TS, Nystrom LE, Noll DC, Jonides J, et al. Temporal dynamics of brain activation during a working memory task. Nature. 1997; 386(6625):604–608. [PubMed: 9121583]

Cox RW. AFNI: software for analysis and visualization of functional magnetic resonance neuroimages. Comput Biomed Res. 1996; 29(3):162–173. [PubMed: 8812068]

Dai W, Garcia D, de Bazelaire C, Alsop DC. Continuous flow-driven inversion for arterial spin labeling using pulsed radio frequency and gradient fields. Magn Reson Med. 2008; 60(6):1488–1497. [PubMed: 19025913]

Detre JA, Leigh JS, Williams DS, Koretsky AP. Perfusion imaging. Magn Reson Med. 1992; 23(1): 37–45. [PubMed: 1734182]

Duong TQ, Kim DS, Ugurbil K, Kim SG. Localized cerebral blood flow response at submillimeter columnar resolution. Proc Natl Acad Sci U S A. 2001; 98(19):10904–10909. [PubMed: 11526212]

Fleisher AS, Podraza KM, Bangen KJ, Taylor C, Sherzai A, Sidhar K, et al. Cerebral perfusion and oxygenation differences in Alzheimer's disease risk. Neurobiol Aging. 2009; 30(11):1737–1748. [PubMed: 18325636]

Fox MD, Snyder AZ, Vincent JL, Corbetta M, Van Essen DC, Raichle ME. The human brain is intrinsically organized into dynamic, 0anticor-related functional networks. Proc Natl Acad Sci U S A. 2005; 102(27):9673–9678. [PubMed: 15976020]

Garraux G, Hallett M, Talagala SL. CASL fMRI of subcortico-cortical perfusion changes during memory-guided finger sequences. Neuroimage. 2005; 25(1):122–132. [PubMed: 15734349]

Greicius MD, Krasnow B, Reiss AL, Menon V. Functional connectivity in the resting brain: a network analysis of the default mode hypothesis. Proc Natl Acad Sci U S A. 2003; 100(1):253–258. [PubMed: 12506194]

Hampson M, Driesen NR, Skudlarski P, Gore JC, Constable RT. Brain connectivity related to working memory performance. J Neurosci. 2006; 26(51):13338–13343. [PubMed: 17182784]

Jansma JM, Ramsey NF, Coppola R, Kahn RS. Specific versus nonspecific brain activity in a parametric N-back task. Neuroimage. 2000; 12(6):688–697. [PubMed: 11112400]

Jonides J, Schumacher EH, Smith EE, Lauber EJ, Awh E, Minoshima S, et al. Verbal Working Memory Load Affects Regional Brain Activation as Measured by PET. Journal of Cognitive Neuroscience. 1997; 9(4):462–475. [PubMed: 23968211]

Kensinger EA, Shearer DK, Locascio JJ, Growdon JH, Corkin S. Working memory in mild Alzheimer's disease and early Parkinson's disease. Neuropsychology. 2003; 17(2):230–239. [PubMed: 12803428]

Kim J, Whyte J, Wang J, Rao H, Tang KZ, Detre JA. Continuous ASL perfusion fMRI investigation of higher cognition: quantification of tonic CBF changes during sustained attention and working memory tasks. Neuroimage. 2006; 31(1):376–385. [PubMed: 16427324]

Kirschen MP, Chen SH, Schraedley-Desmond P, Desmond JE. Load- and practice-dependent increases in cerebro-cerebellar activation in verbal working memory: an fMRI study. Neuroimage. 2005; 24(2):462–472. [PubMed: 15627588]

Lim J, Wu WC, Wang J, Detre JA, Dinges DF, Rao H. Imaging brain fatigue from sustained mental workload: an ASL perfusion study of the time-on-task effect. Neuroimage. 2010; 49(4):3426–3435. [PubMed: 19925871]

Lin P, Hasson U, Jovicich J, Robinson S. A neuronal basis for task-negative responses in the human brain. Cereb Cortex. 2011; 21(4):821–830. [PubMed: 20805236]

Luh WM, Wong EC, Bandettini PA, Ward BD, Hyde JS. Comparison of simultaneously measured perfusion and BOLD signal increases during brain activation with T(1)-based tissue identification. Magn Reson Med. 2000; 44(1):137–143. [PubMed: 10893532]

Mazoyer B, Zago L, Mellet E, Bricogne S, Etard O, Houde O, et al. Cortical networks for working memory and executive functions sustain the conscious resting state in man. Brain Res Bull. 2001; 54(3):287–298. [PubMed: 11287133]

McKiernan KA, Kaufman JN, Kucera-Thompson J, Binder JR. A parametric manipulation of factors affecting task-induced deactivation in functional neuroimaging. J Cogn Neurosci. 2003; 15(3): 394–408. [PubMed: 12729491]

Mildner T, Trampel R, Moller HE, Schafer A, Wiggins CJ, Norris DG. Functional perfusion imaging using continuous arterial spin labeling with separate labeling and imaging coils at 3 T. Magn Reson Med. 2003; 49(5):791–795. [PubMed: 12704759]

Miller KL, Luh WM, Liu TT, Martinez A, Obata T, Wong EC, et al. Nonlinear temporal dynamics of the cerebral blood flow response. Hum Brain Mapp. 2001; 13(1):1–12. [PubMed: 11284042]

Ogawa S, Menon RS, Tank DW, Kim SG, Merkle H, Ellermann JM, et al. Functional brain mapping by blood oxygenation level-dependent contrast magnetic resonance imaging. A comparison of signal characteristics with a biophysical model. Biophys J. 1993; 64(3):803–812.

Olson IR, Rao H, Moore KS, Wang J, Detre JA, Aguirre GK. Using perfusion fMRI to measure continuous changes in neural activity with learning. Brain Cogn. 2006; 60(3):262–271. [PubMed: 16423439]

Owen AM, McMillan KM, Laird AR, Bullmore E. N-back working memory paradigm: a meta-analysis of normative functional neuroimaging studies. Hum Brain Mapp. 2005; 25(1):46–59. [PubMed: 15846822]

Pfefferbaum A, Chanraud S, Pitel AL, Muller-Oehring E, Shankaranarayanan A, Alsop DC, et al. Cerebral blood flow in posterior cortical nodes of the default mode network decreases with task engagement but remains higher than in most brain regions. Cereb Cortex. 2011; 21(1):233–244. [PubMed: 20484322]

Poline JB, Worsley KJ, Evans AC, Friston KJ. Combining spatial extent and peak intensity to test for activations in functional imaging. Neuroimage. 1997; 5(2):83–96. [PubMed: 9345540]

Raichle ME. Neuroscience. The brain's dark energy. Science. 2006; 314(5803):1249–1250.

Raichle ME, MacLeod AM, Snyder AZ, Powers WJ, Gusnard DA, Shulman GL. A default mode of brain function. Proc Natl Acad Sci U S A. 2001; 98(2):676–682. [PubMed: 11209064]

Raichle ME, Mintun MA. Brain work and brain imaging. Annu Rev Neurosci. 2006; 29:449–476. [PubMed: 16776593]

Rao H, Wang J, Tang K, Pan W, Detre JA. Imaging brain activity during natural vision using CASL perfusion fMRI. Hum Brain Mapp. 2007; 28(7):593–601. [PubMed: 17034034]

Shulman GL, Fiez JA, Corbetta M, Buckner RL, Miezin FM, Raichle ME, et al. Common blood flow changes across visual tasks: II. Decreases in cerebral cortex. J Cogn Neurosci. 1997; 9(5):16.

Talagala SL, Noll DC. Functional MRI using steady-state arterial water labeling. Magn Reson Med. 1998; 39(2):179–183. [PubMed: 9469699]

Tomasi D, Ernst T, Caparelli EC, Chang L. Common deactivation patterns during working memory and visual attention tasks: an intra-subject fMRI study at 4 Tesla. Hum Brain Mapp. 2006; 27(8): 694–705. [PubMed: 16404736]

Valera EM, Faraone SV, Biederman J, Poldrack RA, Seidman LJ. Functional neuroanatomy of working memory in adults with attention-deficit/hyperactivity disorder. Biol Psychiatry. 2005; 57(5):439–447. [PubMed: 15737657]

Veltman DJ, Rombouts SA, Dolan RJ. Maintenance versus manipulation in verbal working memory revisited: an fMRI study. Neuroimage. 2003; 18(2):247–256. [PubMed: 12595179]

Wang J, Aguirre GK, Kimberg DY, Detre JA. Empirical analyses of null-hypothesis perfusion FMRI data at 1.5 and 4 T. Neuroimage. 2003; 19(4):1449–1462. [PubMed: 12948702]

Wang J, Aguirre GK, Kimberg DY, Roc AC, Li L, Detre JA. Arterial spin labeling perfusion fMRI with very low task frequency. Magn Reson Med. 2003; 49(5):796–802. [PubMed: 12704760]

Wang J, Li L, Roc AC, Alsop DC, Tang K, Butler NS, et al. Reduced susceptibility effects in perfusion fMRI with single-shot spin-echo EPI acquisitions at 1.5 Tesla. Magn Reson Imaging. 2004; 22(1):1–7. [PubMed: 14972387]

Wang J, Rao H, Wetmore GS, Furlan PM, Korczykowski M, Dinges DF, et al. Perfusion functional MRI reveals cerebral blood flow pattern under psychological stress. Proc Natl Acad Sci U S A. 2005; 102(49):17804–17809. [PubMed: 16306271]

Wang J, Zhang Y, Wolf RL, Roc AC, Alsop DC, Detre JA. Amplitude-modulated continuous arterial spin-labeling 3.0-T perfusion MR imaging with a single coil: feasibility study. Radiology. 2005; 235(1):218–228. [PubMed: 15716390]

Williams DS, Detre JA, Leigh JS, Koretsky AP. Magnetic resonance imaging of perfusion using spin inversion of arterial water. Proc Natl Acad Sci U S A. 1992; 89(1):212–216. [PubMed: 1729691]

Wu WC, Fernandez-Seara M, Detre JA, Wehrli FW, Wang J. A theoretical and experimental investigation of the tagging efficiency of pseudocontinuous arterial spin labeling. Magn Reson Med. 2007; 58(5):1020–1027. [PubMed: 17969096]

Xu G, Rowley HA, Wu G, Alsop DC, Shankaranarayanan A, Dowling M, et al. Reliability and precision of pseudo-continuous arterial spin labeling perfusion MRI on 3.0 T and comparison with 15O-water PET in elderly subjects at risk for Alzheimer's disease. NMR Biomed. 2010; 23(3): 286–293. [PubMed: 19953503]

Yang Y, Engelien W, Pan H, Xu S, Silbersweig DA, Stern E. A CBF-based event-related brain activation paradigm: characterization of impulse-response function and comparison to BOLD. Neuroimage. 2000; 12(3):287–297. [PubMed: 10944411]

Ye FQ, Berman KF, Ellmore T, Esposito G, van Horn JD, Yang Y, et al. H(2)(15)O PET validation of steady-state arterial spin tagging cerebral blood flow measurements in humans. Magn Reson Med. 2000; 44(3):450–456. [PubMed: 10975898]

Ye FQ, Smith AM, Mattay VS, Ruttimann UE, Frank JA, Weinberger DR, et al. Quantitation of regional cerebral blood flow increases in prefrontal cortex during a working memory task: a steady-state arterial spin-tagging study. Neuroimage. 1998; 8(1):44–49. [PubMed: 9698574]

Yee SH, Liu HL, Hou J, Pu Y, Fox PT, Gao JH. Detection of the brain response during a cognitive task using perfusion-based event-related functional MRI. Neuroreport. 2000; 11(11):2533–2536. [PubMed: 10943717]

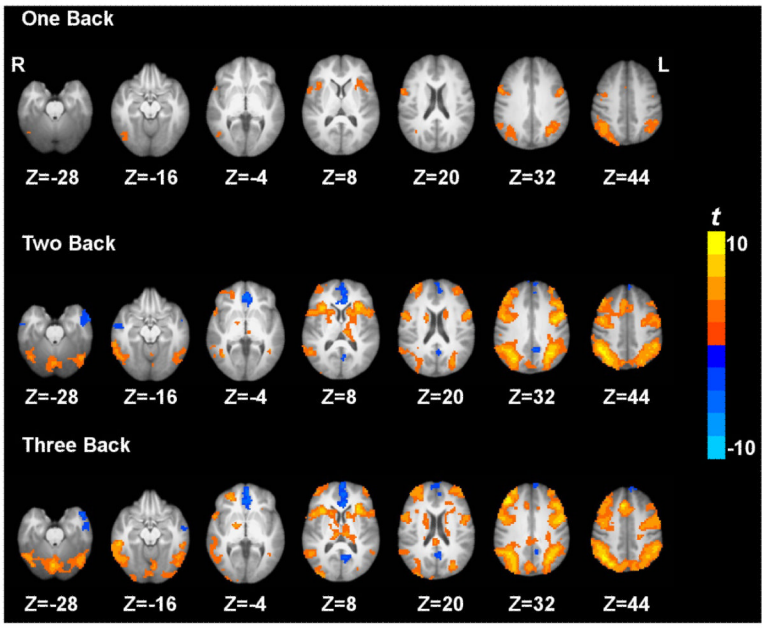

Figure 1.
Paired *t*-maps between the three active working memory task conditions and the 0 back baseline vigilance task condition based on quantified CBF. $p < 0.05$ corrected. 'L' denotes the left hemisphere of the brain and 'R' denotes the right hemisphere.

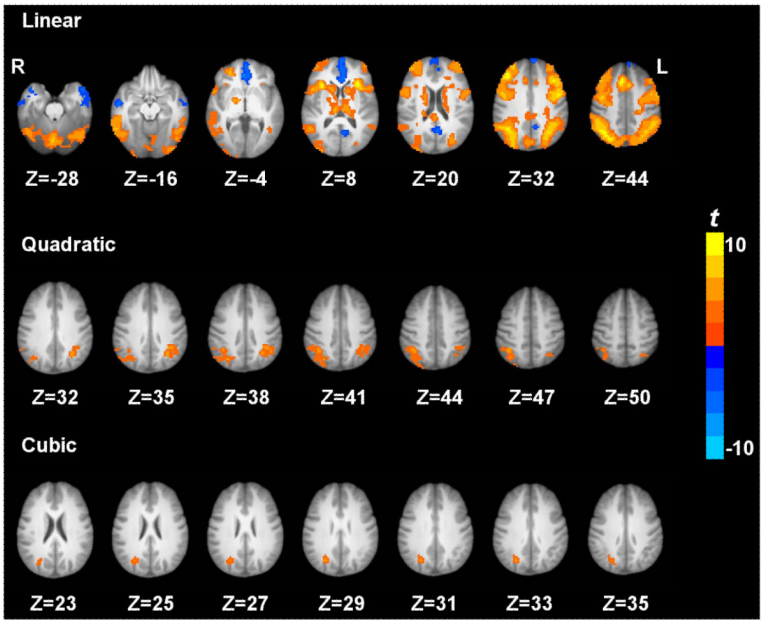

Figure 2.
Trend *t*-maps across the four working memory conditions based on quantified CBF. $p < 0.05$ corrected. 'L' denotes the left hemisphere of the brain and 'R' denotes the right hemisphere.

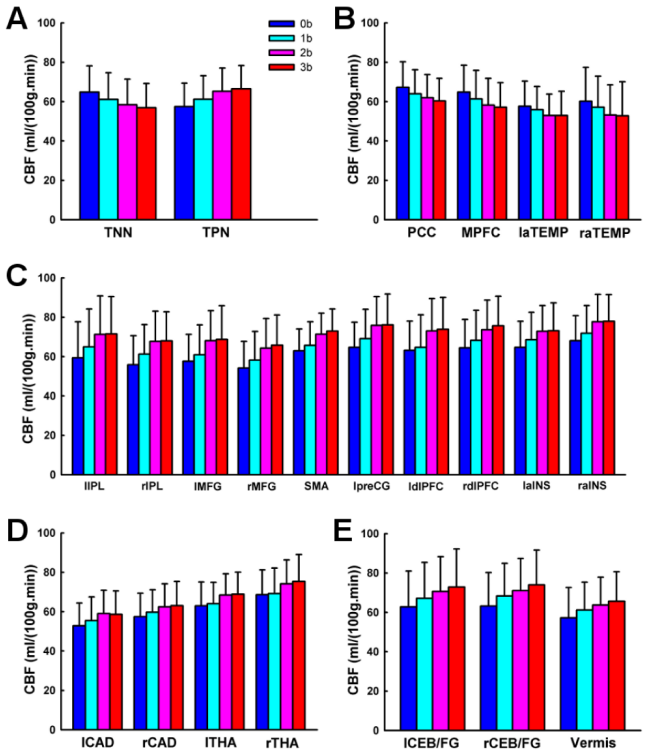

Figure 3.

The average quantitative CBF values in the TNN and TPN ROIs (A), in the ROIs which exhibited linearly decreasing CBF (B), in the cortical ROIs which exhibited linearly increasing CBF (C), in the subcortical ROIs which exhibited linearly increasing CBF (D), and in the cerebellar ROIs which exhibited linearly increasing CBF (E) from 0b to 3b. Bars labeled in blue, cyan, pink and red demonstrate the CBF values under 0b, 1b, 2b and 3b, separately. TNN: task negative network; TPN: task positive network. PCC: posterior cingulate cortex; MPFC: medial prefrontal cortex; laTEMP: left anterior temporal gyrus; raTEMP: right anterior temporal gyrus. lIPL: left inferior parietal lobule. rIPL: right inferior parietal lobule. lMFG: left middle frontal gyrus; rMFG: right middle frontal gyrus; SMA: supplementary motor area; lpreCG: left precentral cingulate gyrus; ldlPFC: left dorsolateral prefrontal cortex; rdlPFC: right dorsolateral prefrontal cortex; laINS: left anterior insula; raINS: right anterior insula. lCAD: left caudate; rCAD: right CAD; lTHA: left thalamus; rTHA: right thalamus. lCEB/FG: left cerebellum/fusiform gyrus; rCEB/FG: right cerebellum/fusiform gyrus.

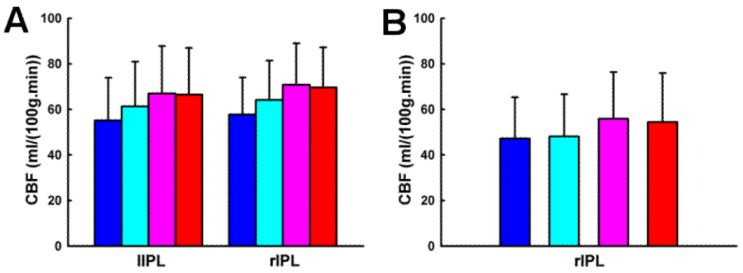

Figure 4.

The average quantitative CBF values in the cortical ROIs exhibiting a quadratic trend of CBF (A) and in the cortical ROIs exhibiting a cubic trend of CBF (B) from 0b to 3b. Bars labeled in blue, cyan, pink and red demonstrate the CBF values under 0b, 1b, 2b and 3b, separately. lIPL: left inferior parietal lobule. rIPL: right inferior parietal lobule.

Table 1

Behavior data of the four working memory task loads

Task Load	hit rate (mean ± S.D.)	false alarm rate (mean ± S.D.)	dprime (mean ± S.D.)
0b	0.99 ± 0.03	0.01 ± 0.005	4.69 ± 0.42
1b	0.92 ± 0.08	0.03 ± 0.03	3.76 ± 0.84
2b	0.85 ± 0.11	0.06 ± 0.05	2.91 ± 0.79
3b	0.68 ± 0.13	0.06 ± 0.05	2.21 ± 0.63

Table 2

Quantitative CBF of the whole brain

Task Load	Quantitative CBF (mean ± S.D.)
0b	48.58 ± 9.34
1b	49.81 ± 9.15
2b	49.82 ± 9.08
3b	50.61 ± 8.75